

Magnetization symmetry for the MnTe altermagnetic candidate

N.N. Orlova,¹ V.D. Esin,¹ A.V. Timonina,¹ N.N. Kolesnikov,¹ and E.V. Deviatov¹

¹*Institute of Solid State Physics of the Russian Academy of Sciences,
Chernogolovka, Moscow District, 2 Academician Ossipyan str., 142432 Russia*

(Dated: February 18, 2025)

We experimentally investigate the magnetization angle dependence $M(\alpha)$ for single crystals of MnTe altermagnetic candidate. In high magnetic fields, experimental $M(\alpha)$ curves nearly independent of temperature, they mostly reflect standard antiferromagnetic spin-flop processes below the Néel vector reorientation field. In contrast, $M(\alpha)$ dependences are quite unusual at low temperatures and in low magnetic fields: below 81 K, spontaneous magnetization appears as a sharp $M(T)$ magnetization jump, the easy axis direction is equally $\pi/2$ rotated either by increasing the field above 1 kOe or the temperature above 81 K. We provide experimental arguments that the spontaneous magnetization of MnTe below 81 K differs strongly from the well known weak ferromagnetism of conventional antiferromagnetics, thus, it requires to take into account formation of the altermagnetic ground state. Despite the MnTe altermagnetic state is expected to be g-wave, i.e. $\pi/3$ periodic one, our experiment confirms the prevailing population of one from three easy axes, as it has been shown previously by temperature-dependent angle-resolved photo-emission spectroscopy.

I. INTRODUCTION

Recently, a new class of altermagnetic materials has been added to usual ferro- and antiferro- magnetic classes^{1,2}. Normally, ferromagnetic and antiferromagnetic materials belong to the nonrelativistic groups of magnetic symmetry, i.e. to the case of weak spin-orbit coupling. In contrast, topological materials are always characterized by strong spin-orbit interaction³⁻⁵, and, therefore, by spin-momentum locking⁶. For example, spin is rotating along the Fermi-arc in Weyl semimetals⁷, while the drumhead surface states lead to the spin textures of the skyrmion type in topological nodal-line semimetals⁸.

In altermagnets, the concept of spin-momentum locking⁶ was extended to the non-relativistic groups of magnetic symmetry^{1,2}. As a result, the small net magnetization is accompanied by alternating spin splitting in the k-space^{1,9}. For example, for the d-wave altermagnet¹⁰ the up-polarized subband can be obtained by $\pi/2$ rotation of the down-polarized one in the k-space^{11,12}. For other altermagnets, it can be also expected g- or even i-wave order parameters¹, despite it is still an open question to verify these predictions experimentally. For example, it was even proposed to address the k-space spin polarization by interfacing an altermagnet with the surface of a topological insulator¹³.

Anomalous Hall effect⁵ was theoretically predicted¹⁴ and experimentally demonstrated^{10,15-17} for altermagnets. In contrast to RuO₂ altermagnetic candidate¹⁰, the measurements in MnTe and Mn₅Si₃ show hysteresis and spontaneous AHE signals at zero magnetic field¹⁵⁻¹⁷. It is a common agreement, that AHE still requires finite net magnetization¹⁸ and spin-orbit coupling also in altermagnetic materials^{15,16,19}. The AHE transverse current is usually assumed to be perpendicular to magnetization, therefore, AHE and the ferromagnetic spin moment share the same symmetry. However, it is not generally so in materials with weak net magnetization^{19,20}. For

example, the AHE signal does not correlate with the angle dependence of the weak saturation magnetization for Mn₅Si₃¹⁷.

On the other hand, the order parameter is defined by the Néel vector symmetry in altermagnets¹, so the expected d-, g- or i-wave symmetry could be observable in magnetization measurements. This investigation can be conveniently performed for MnTe²¹, which is characterized by accessible (2–3 T) magnetic field range^{15,16} in contrast to RuO₂¹⁰ altermagnetic candidate.

MnTe is an intrinsic room-temperature magnetic semiconductor with antiparallel magnetic ordering of Mn moments¹⁵. In detail, the magnetic moments on Mn have a parallel alignment within the c planes and an antiparallel alignment between the planes, so the two magnetic sublattices are connected by a sixfold screw axis along [0001]. As an altermagnetic candidate, MnTe is expected to have g-wave order parameter^{1,22}, although it is still debatable in recent publications²³.

Despite the long history of investigations²⁴⁻²⁹, the experimental data on the magnetization angle dependence are quite controversial for MnTe. For example, MnTe is of hexagonal NiAs structure, but $\pi/3$ periodicity has only been demonstrated in high magnetic fields (much above 2 T) by torque technique³⁰ and by magnetoresistance measurements³¹. In the latter case, magnetoresistance could directly reflect the crystal symmetry due to the scattering anisotropy, while magnetization was only investigated for two perpendicular directions³¹. Also, MnTe shows spontaneous ferromagnetic-like magnetization at low temperatures³², which is quite unusual for collinear antiferromagnetics. Thus, to conclude on the symmetry of the altermagnetic order parameter, it is reasonable to investigate the MnTe magnetization angle dependence in a wide field range.

Here, we experimentally investigate the magnetization angle dependence $M(\alpha)$ for single crystals of MnTe altermagnetic candidate. In high magnetic fields, experimental $M(\alpha)$ curves nearly independent of temperature, they

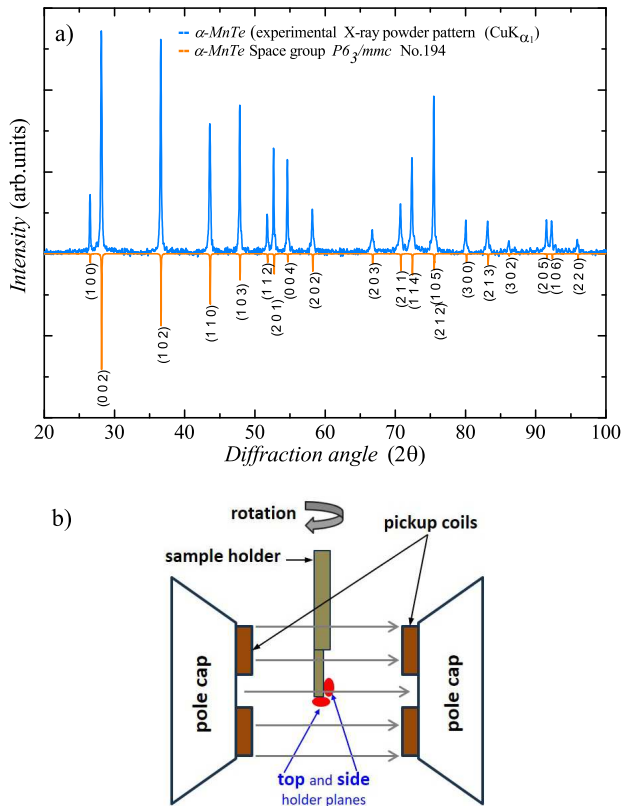


FIG. 1. (Color online) (a) The X-ray powder diffraction pattern (Cu $K_{\alpha 1}$ radiation), which is obtained for the crushed MnTe single crystal. The single-phase α -MnTe is confirmed with the space group $P6_3/mmc$ No. 194, so the results below cannot appear from the incorrect stoichiometry or oxides. (b) Schematic diagram of the experimental setup, with mutual orientation of the magnetic field, sample holder rotation axis and the magnetometer detector coils. The magnetometer detector coils are fixed to the magnet pole caps, so $M(\alpha)$ angle-dependent magnetization does not change a sign in constant magnetic field. The sample can be mounted to the side or the top sample holder planes, to vary MnTe sample orientation in respect to the magnetic field and the rotation axis.

mostly reflect standard antiferromagnetic spin-flop processes below the Néel vector reorientation field. In contrast, $M(\alpha)$ dependences are quite unusual at low temperatures and in low magnetic fields: below 81 K, spontaneous magnetization appears as a sharp $M(T)$ magnetization jump, the easy axis direction is equally $\pi/2$ rotated either by increasing the field above 1 kOe or the temperature above 81 K.

II. SAMPLES AND TECHNIQUE

To investigate magnetization anisotropy for α -MnTe, it is preferable to use small MnTe single crystal samples rather than thin films. In the latter case, the results may

be seriously affected by the geometrical factors and by the admixture of the substrate magnetic response, especially in low magnetic fields³¹. For this reason, we investigate small (2 mg – 6 mg mass) mechanically cleaved single crystal MnTe samples.

α -MnTe was synthesized by reaction of elements (99.99% Mn and 99.9999% Te) in evacuated silica ampules slowly heated up to 1050–1070°C. The obtained loads were melted in the graphite crucibles under 10 MPa argon pressure, then homogenized at 1200°C for 1 hour. The crystals grown by gradient freezing method are groups of single crystal domains with volume up to 0.5–1.0 cm³. The MnTe composition is verified by energy-dispersive X-ray spectroscopy. The powder X-ray diffraction analysis confirms single-phase α -MnTe with the space group $P6_3/mmc$ No. 194, see Fig. 1 (a).

Sample magnetization is measured by Lake Shore Cryotronics 8604 VSM magnetometer, equipped with nitrogen flow cryostat. The magnetization anisotropy $M(\alpha)$ is investigated by sample holder rotation in the external magnetic field, see Fig. 1 (b). The magnetometer detector coils are fixed to the magnet pole caps, so $M(\alpha)$ angle-dependent magnetization does not change a sign in constant magnetic field³². Also, the sample can be mounted to either the side or the top sample holder planes in Fig. 1 (b), to vary MnTe sample orientation in respect to the magnetic field and the rotation axis. Since for MnTe there is no definite cleavage plane, the initial orientation of the MnTe single crystal should be obtained from experimental $M(\alpha)$ curves.

The sample is mounted to the sample holder by low temperature grease. It is verified³³, that without MnTe sample, the sample holder with corresponding amount of grease shows fully isotropic and strictly linear diamagnetic response, which can be estimated as below 10% of the measured MnTe magnetization value. Before any measurements, the sample is cooled down the minimal 78 K temperature in zero magnetic field. Afterward, the sample is magnetized at 15 kOe, to have the stable, well-reproducible initial sample state. Thus, the experimental setup allows to obtain magnetization angle dependence with high resolution in a wide magnetic field range ± 15 kOe.

III. EXPERIMENTAL RESULTS

Fig. 2 shows $M(H)$ and $M(\alpha)$ magnetization dependences for the 2.89 mg MnTe sample. The sample is mounted to the side plane of the holder, as depicted in Fig. 1 (b).

The insert to Fig. 2 (a) shows the $M(\alpha)$ angle dependence of magnetization, obtained for 200 Oe magnetic field at 78 K temperature. $M(\alpha)$ is of π periodicity, it shows two maxima ($\alpha = 170^\circ$ and π -shifted) and two minima ($\alpha = 80^\circ$ and π -shifted).

The main plot of Fig. 2 (a) shows $M(H)$ field-dependent sample magnetization within ± 15 kOe field

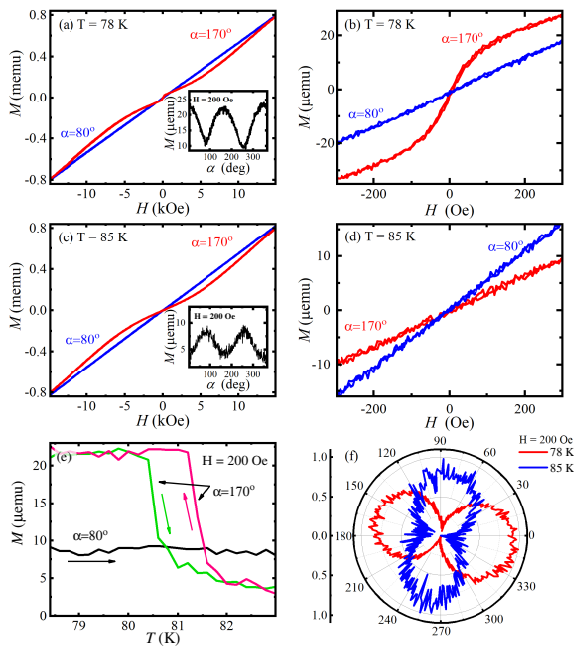


FIG. 2. (Color online) $M(H)$ and $M(\alpha)$ magnetization dependences for the 2.89 mg MnTe sample. The sample is mounted to the side plane of the holder. (a) $M(H)$ field-dependent magnetization within ± 15 kOe field range at 78 K temperature. The curves are for $M(\alpha)$ maximum (the red curve, $\alpha = 170^\circ$) and minimum (the blue curve, $\alpha = 80^\circ$). The blue curve is strictly linear, while there are nonlinear $M(H)$ branches with zero-field kink for the red one. Insert shows $M(\alpha)$ angle dependence of magnetization, obtained for 200 Oe magnetic field at 78 K temperature. (b) The low-field $M(H)$ behavior at 78 K temperature, the curves are obtained with high accuracy and with smaller magnetic field step. They confirm ferromagnetic-like hysteresis at $\alpha = 170^\circ$ (the red curve). (c) and (d) Similarly obtained $M(H)$ curves at 85 K temperature. $M(\alpha)$ is still π periodic, see the inset, but the maxima and the minima positions are interchanged at 85 K in comparison with 78 K temperature in the inset to Fig. 2 (a). Also, $M(H)$ is strictly linear in low fields for both field orientations, so the low-field hysteresis disappears at 85 K, see Fig. 2 (d). At higher fields, there are nonlinear $M(H)$ branches for $\alpha = 170^\circ$, which now corresponds to the $M(\alpha)$ minimum, while $M(H)$ is strictly linear for $\alpha = 80^\circ$ (the blue curve). (e) The detailed temperature dependences for two orientations of 200 Oe magnetic field: green and pink curves are obtained at $\alpha = 170^\circ$, for heating and cooling, respectively, while the black one is for $\alpha = 80^\circ$. Ferromagnetic-like spontaneous magnetization appears as a sharp $M(T)$ jump. (f) The normalized $\Delta M(\alpha)/M$ is shown as the circular diagram at 200 Oe magnetic field for two, 78 K and 85 K, temperatures. As the most important result, the easy axis is $\pi/2$ rotated when spontaneous ferromagnetic-like magnetization is destroyed above 81 K.

range at 78 K temperature. $M(H)$ is measured by standard method of the magnetic field gradual sweeping between two opposite field values to obtain $M(H)$ magnetization loops at fixed angle α . The curves are for $M(\alpha)$ maximum (the red curve, $\alpha = 170^\circ$) and minimum (the blue curve, $\alpha = 80^\circ$). $M(H)$ is strictly linear for $M(\alpha)$ minimum (the blue curve), without any peculiarities. In contrast, for $\alpha = 170^\circ$ there are nonlinear $M(H)$ branches with pronounced zero-field kink³² (the

red curve). The low-field region is shown in Fig. 2 (b), the curves are obtained with high accuracy and with smaller magnetic field step. They confirm ferromagnetic-like hysteresis at $\alpha = 170^\circ$ (the red curve) and strictly linear $M(H)$ at $\alpha = 80^\circ$ (the blue curve). Thus, at 78 K the low-field magnetization shows π -periodic easy-axis magnetic anisotropy.

Figs. 2 (c) and (d) shows similarly obtained $M(H)$ curves at 85 K temperature. $M(\alpha)$ is still π periodic, see the inset to Fig. 2 (c), but the maxima and the minima positions are interchanged at 85 K in comparison with 78 K temperature in the inset to Fig. 2 (a). Also, $M(H)$ is strictly linear in low fields for both field orientations, so the low-field hysteresis disappears at 85 K, see Fig. 2 (d). At higher fields, there are nonlinear $M(H)$ branches for $\alpha = 170^\circ$, which now corresponds to the $M(\alpha)$ minimum, while $M(H)$ is strictly linear for $\alpha = 80^\circ$ (the blue curve).

The detailed $M(T)$ temperature dependence is shown in Fig. 2 (e) for two above mentioned orientations of the 200 Oe magnetic field, the temperature is stabilized with 0.2 K step from 78.4 K to 83 K. Green and pink curves are obtained at $\alpha = 170^\circ$, for heating and cooling, respectively, while the black one is linear at $\alpha = 80^\circ$. It can be seen from Fig. 2 (e), that ferromagnetic-like spontaneous magnetization appears below 80.5–81.5 K at $\alpha = 170^\circ$ as a sharp $M(T)$ jump, which is quite unusual for standard ferromagnetic transitions.

$M(\alpha)$ results are summarized as the circular diagram in Fig. 2 (f). The normalized $\Delta M/M$ is shown as a bar plot in polar coordinates at 200 Oe magnetic field for two, 78 K and 85 K, temperatures. Both the π -like periodicity and the easy-axis direction can be clearly seen from the diagram. As the most important result, the easy axis is $\pi/2$ rotated when spontaneous ferromagnetic-like magnetization is destroyed above 81 K.

Fig. 3 shows evolution of $M(\alpha)$ angular dependence of magnetization with magnetic field at two 78 K and 85 K temperatures, to both sides of the $M(T)$ jump at 81 K. The $M(\alpha)$ curves are shown with the 0.2–0.3 kOe step from 0 to the 1 kOe magnetic field and with the 1.5–2 kOe step for the higher fields.

For the magnetic field from 2.5 kOe to 15 kOe, the experimental $M(\alpha)$ curves nearly coincide at 78 K and at 85 K temperatures, see Figs. 3 (a) and (b), respectively. We observe π -periodicity of the curves for the 2.5 kOe to 10 kOe field range, while it is changed to the $\pi/2$ -one with two additional maxima at higher fields.

Below 1 kOe, $M(\alpha)$ is of different behavior for 78 K and for 85 K temperatures in Figs. 3 (a) and (b). At high 85 K temperature in Fig. 3 (b), $M(\alpha)$ is always π -periodic, the maxima and minima positions are stable in the full field range. In contrast, at 78 K temperature $M(\alpha)$ is just inverted for 0.2–0.8 kOe magnetic fields in Fig. 3 (a), as it is described above.

At zero magnetic field, the remanence magnetization vanishes at 85 K temperature in Fig. 3 (b), while it clearly oscillates at 78 K in Fig. 3 (a): without the external field,

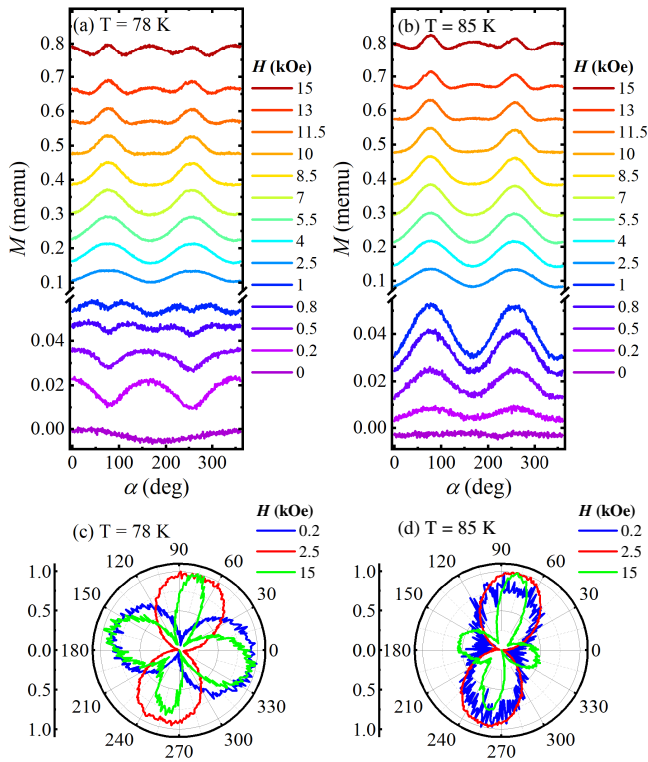


FIG. 3. (Color online) The detailed $M(\alpha)$ magnetization dependences for the 2.89 mg MnTe sample at two, 78 K and 85 K, temperatures. (a) and (b) The $M(\alpha)$ curves are shown with the 0.2–0.3 kOe step from 0 to the 1 kOe field value and with the 1.5–2 kOe step for the high, 1 to 15 kOe field range. From 2.5 kOe to 15 kOe, the experimental $M(\alpha)$ curves nearly coincide at 78 K and at 85 K temperatures in (a) and (b), respectively. Below 1 kOe, $M(\alpha)$ is of different behavior: at 85 K temperature, $M(\alpha)$ is always π -periodic, the maxima positions are stable in the full field range. In contrast, at 78 K temperature $M(\alpha)$ is inverted for the 0.2 kOe - 0.8 kOe magnetic fields. (c) and (d) Circular diagrams for the characteristic field values 0.2 kOe, 2.5 kOe and 15 kOe at 78 K and at 85 K temperatures in (c) and (d), respectively. For the low-temperature low-field ferromagnetic-like state, the easy axis direction is equally $\pi/2$ rotated either by increasing the field above 1 kOe in (c) or the temperature above 81 K in (d).

constant sample magnetization produces 2π -periodic oscillating signal in the magnetometer detector coils.

These $M(\alpha)$ data are summarized in the circular diagrams for the characteristic field values 0.2 kOe, 2.5 kOe and 15 kOe, see Figs. 3 (c) and (d). While increasing magnetic field from 0.2 kOe to 2.5 kOe in Fig. 3 (c), the easy magnetization axis is rotating on the $\pi/2$ angle at 78 K. In contrast, the easy axis direction is stable at 85 K in Fig. 3 (d). At 15 kOe field, $M(\alpha)$ is of identical $\pi/2$ -symmetry at both temperatures.

Thus, for the low-temperature low-field ferromagnetic-like state, the easy axis direction is equally $\pi/2$ rotated either by increasing the field above 1 kOe or the temperature above 81 K, see Figs. 2 (f) and 3 (c-d).

To change the MnTe sample orientation in respect to

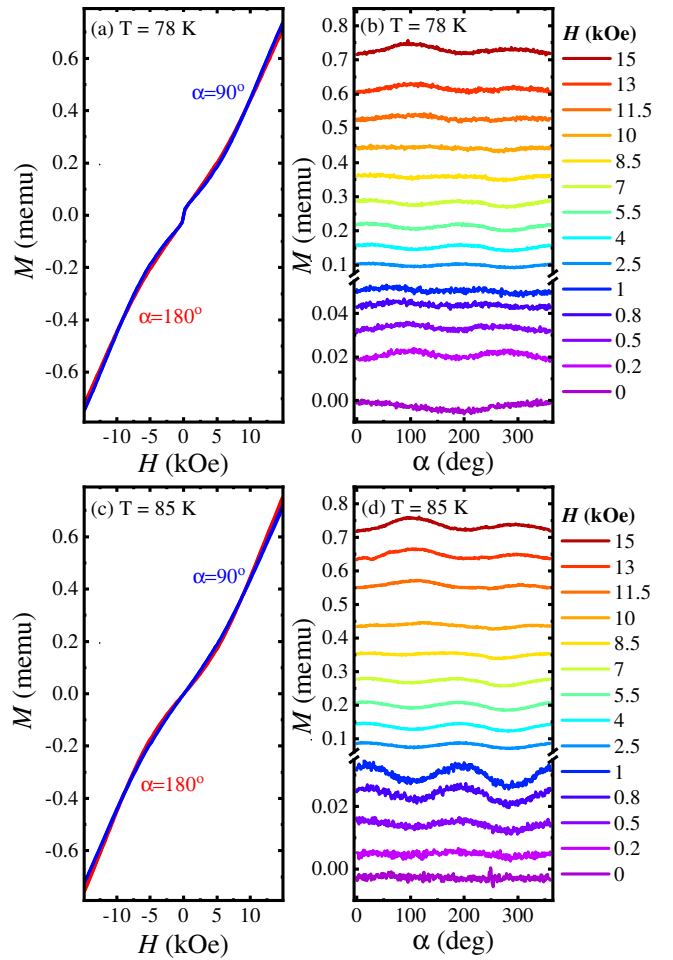


FIG. 4. (Color online) $M(H)$ and $M(\alpha)$ magnetization dependences for the 2.89 mg MnTe sample. The sample is fixed to the top holder plane by the same crystal surface, as depicted in Fig. 1 (b). In general, the low-field behavior is equivalent for both sample orientations: the π -periodic $M(\alpha)$ oscillations are inverted at 78 K and 85 K, so the easy axis is equally $\pi/2$ rotated either by increasing the field to 2.5 kOe or the temperature to 85 K. (a) $M(H)$ field-dependent magnetization within ± 15 kOe field range at 78 K temperature. The curves are equally nonlinear for $\alpha = 180^\circ$ (the red curve) and $\alpha = 90^\circ$ (the blue curve), so the magnetic field is always within the MnTe basal plane. The low-field hysteresis is also present for both angles. (b) $M(\alpha)$ curves at 78 K with the 0.2–0.3 kOe step from 0 to the 1 kOe field and with the 1.5–2 kOe step for higher fields. (c) $M(H)$ field-dependent magnetization within ± 15 kOe field range at 85 K temperature. The curves are for $\alpha = 180^\circ$ (the red curve) and $\alpha = 90^\circ$ (the blue curve), the low-field hysteresis is suppressed. (d) Similarly obtained $M(\alpha)$ curves at 85 K.

the magnetic field and the rotation axis, the sample is fixed to the top holder plane by the same crystal surface, as depicted in Fig. 1 (b). The $M(H)$ and $M(\alpha)$ dependences are presented in Fig. 4. From these data, external magnetic field is always within the Néel vector coplanar plane (the MnTe basal plane): the high-field $M(H)$

branches are equally nonlinear for any angle α , so the magnetic field is always normal to the MnTe c -axis, i.e. it is within the MnTe basal plane³⁴. The overall $M(\alpha)$ oscillation amplitude is an order of magnitude smaller, there is no $\pi/2$ $M(\alpha)$ periodicity in high magnetic fields in Fig. 4 (b) and (d).

In general, the low-field behavior is equivalent for both sample orientations: there is no remanence magnetization at 85 K in Fig. 4 (d), while it oscillates at 78 K in Fig. 4 (b). The low-field hysteresis is also present for any rotation angle in Fig. 4 (a), it still can be suppressed by temperature in Fig. 4 (c). The π -periodic $M(\alpha)$ oscillations are inverted at 78 K and 85 K Fig. 4 (b) and (d).

The reported behavior is sample-independent, it can be reproduced for any MnTe single crystal sample. For example, Fig. 5 shows $M(H)$ and $M(\alpha)$ magnetization dependences for the 5.73 mg MnTe sample. The results are summarized by circular diagrams in Fig. 5 (a) and (b), for 78 K and 85 K temperatures, respectively. For the low-temperature low-field ferromagnetic-like state, the easy axis is equally $\pi/2$ rotated either by increasing the field above 1 kOe or the temperature above the transition at 81 K.

At low temperatures, we observe nonlinear $M(H)$ curves with kink at zero field in Fig. 5 (c). The latter reflects the low-field hysteresis, as depicted in Fig. 5 (d). These features are suppressed at 85 K temperature in Fig. 5 (e), the transition is shown in Fig. 5 (f) as sharp $M(T)$ drop at 81 K. This drop can be observed both for the $M(T)$ curve at 200 Oe field, and for the remanence magnetization in zero external field.

IV. DISCUSSION

As a result, $M(\alpha)$ is quite unusual at low temperatures and in low magnetic fields: below 81 K, spontaneous magnetization appears, which is accompanied by easy axis rotation over $\pi/2$ in Figs. 2 (f), 3 (c) and (d).

Let us start from the high-field behavior. We argue, that π and $\pi/2$ periodicity in high magnetic fields reflect usual antiferromagnetic spin-flop processes below the Néel vector reorientation field^{31,34}. MnTe is of hexagonal NiAs structure, the magnetic moments on Mn have a parallel alignment within the basal MnTe planes and an antiparallel alignment between the planes, so the two magnetic sublattices are connected by a sixfold screw axis along [0001] c -axis. Usually, the nonlinear $M(H)$ branches are due to the antiferromagnetic domain configuration change, which is allowed for the field within the basal plane³⁴, as it can be seen in Fig. 4. In contrast, $M(H)$ is strictly linear if the magnetic field is directed along the MnTe c -axis in Fig. 2 (a-d), which leads to the π -periodic $M(\alpha)$ for 1 kOe - 10 kOe fields in Fig. 3. For higher fields, spin-flops are also allowed along the c -axis³⁴, which leads to more complicated $\pi/2$ periodicity in Figs. 2 and 3 above 10 kOe.

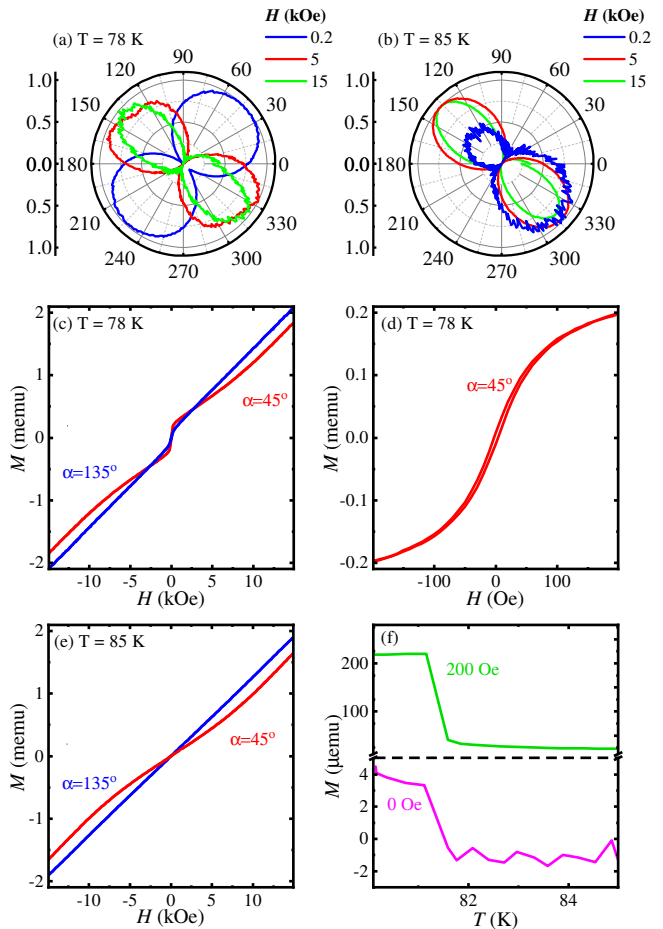


FIG. 5. (Color online) Similar $M(H)$ and $M(\alpha)$ magnetization behavior for the 5.73 mg MnTe sample. (a) and (b) $M(H)$ dependences, summarized as circular diagrams for 78 K and 85 K temperatures, respectively. For the low-temperature low-field ferromagnetic-like state, the easy axis direction is equally $\pi/2$ rotated either by increasing the field above 1 kOe or the temperature above the transition at 81 K. (c) Non-linear $M(H)$ curves with kink at zero field at 78 K temperature for two different angles $\alpha = 135^\circ$ (the blue curve) and $\alpha = 45^\circ$ (the red curve). (d) The low-field $M(H)$ hysteresis at 78 K temperature for $\alpha = 45^\circ$. (e) The hysteresis disappears at 85 K, the high-field $M(H)$ branches are nonlinear for $\alpha = 45^\circ$ (the red curve), while $M(H)$ nearly linear for $\alpha = 135^\circ$ (the blue curve), so the field is parallel to the MnTe c -axis in the latter case. (f) Temperature transition as sharp $M(T)$ drop at 81 K for $\alpha = 45^\circ$. This drop can be observed both at 200 Oe magnetic field (the green curve), and for the remanence magnetization in zero external field (the magenta one).

However, we do not observe $\pi/3$ periodicity of magnetization also in low fields for any sample orientation, despite it should be expected for the hexagonal MnTe structure. This discrepancy can not be connected with any sample disadvantages, like incorrect MnTe stoichiometry, Mn oxides, defects, etc^{35,36}. For our samples, the MnTe composition was verified by energy-dispersive X-

ray spectroscopy and the powder X-ray diffraction analysis. The latter also confirms the space group $P6_3/mmc$ No. 194, see Fig. 1 (a), so one should be sure in $\pi/3$ symmetry for the MnTe basal plane. Moreover, $\pi/3$ periodicity of magnetization has never been demonstrated for MnTe except two high-field experiments^{30,31}.

As a result, the difference between the $M(\alpha)$ magnetization symmetry and the MnTe crystal structure requires to take into account the electronic properties, i.e. formation of the altermagnetic ground state.

MnTe belongs to a new class of altermagnetic materials^{15,16,21}, the small net magnetization is accompanied by alternating spin-momentum locking in the k-space, so the unusual spin splitting is predicted^{1,9}. For the altermagnetic candidate MnTe, it is accepted, that the principle origin of nonzero net magnetic moment^{15,16}, and, therefore of weak remanence magnetization^{19,37} is the spin-orbit coupling¹⁸ in the valence orbitals³⁸. The effects of spin-orbit coupling in this material has been previously investigated by temperature-dependent angle-resolved photo-emission spectroscopy (ARPES) and by disordered local moment calculations³⁹.

In contrast to the expected g-wave MnTe altermagnetic state, our experiment demonstrate $\pi M(\alpha)$ periodicity in low magnetic fields, i.e. d-wave order parameter (see also theoretical discussion in Ref.²³). For the altermagnetic state in bulk MnTe samples, the prevailing population of one from three easy axes has been shown by ARPES⁴⁰. A lower twofold symmetry has therefore been established at energies near the top of the valence band for strong spin-orbit coupling. It seems to be important, that spin-orbit coupling is well-resolved only below 100 K in Ref.³⁹, which is consistent with appearance of spontaneous magnetization in Figs. 2 (e) and 5 (f). Thus, above the 81 K transition temperature or in higher magnetic fields, the easy-axis pinning to the crystal structure is recovered, which is responsible for the easy axis $\pi/2$ rotation either by increasing the field above 1 kOe or the temperature above 80.5–81.5 K in Figs. 2 (f), 3 (c) and (d).

It is important, that spontaneous magnetization of MnTe below 81 K is strongly different from the well known weak ferromagnetism^{41,42} of conventional antiferromagnetics:

- (i) MnTe space group is different from the required for weak ferromagnetism^{42,43}.
- (ii) Weak ferromagnetism originates from the symmetry lowering⁴² in high magnetic fields (above 2 kOe range), it appears as the small, 0.1 %-10 % $M(H)$

jump⁴¹. In contrast, we observe remanence magnetization below 81 K without any external field. Above 1 kOe, the altermagnetic state is destroyed in Figs. 2 (f), 3 (c) and (d). In low 200 Oe field, $M(\alpha)$ modulation is about 50% in Figs. 2 and 3.

(iii) Temperature transition as sharp $M(T)$ jump is very unusual for weak ferromagnetism⁴¹

Thus, despite the ground state symmetry is still debatable in MnTe, the easy axis rotation over $\pi/2$ in Figs. 2 (f), 3 (c) and (d) seems to be the crucial experimental argument for the MnTe altermagnetic ground state below 81 K.

V. CONCLUSION

As a conclusion, we experimentally investigate the magnetization angle dependence $M(\alpha)$ for single crystals of MnTe altermagnetic candidate. In high magnetic fields, experimental $M(\alpha)$ curves nearly independent of temperature, they mostly reflect standard antiferromagnetic spin-flop processes below the Néel vector reorientation field. In contrast, $M(\alpha)$ dependences are quite unusual at low temperatures and in low magnetic fields: below 81 K, spontaneous magnetization appears as a sharp $M(T)$ magnetization jump, the easy axis direction is equally $\pi/2$ rotated either by increasing the field above 1 kOe or the temperature above 81 K. We provide experimental arguments that the spontaneous magnetization of MnTe below 81 K differs strongly from the well known weak ferromagnetism of conventional antiferromagnetics, thus, it requires to take into account formation of the altermagnetic ground state. Despite the MnTe altermagnetic state is expected to be g-wave, i.e. $\pi/3$ periodic one, our experiment confirms the prevailing population of one from three easy axes, as it has been shown previously by temperature-dependent angle-resolved photo-emission spectroscopy.

ACKNOWLEDGMENTS

We wish to thank S.S Khasanov for X-ray sample characterization and Vladimir Zyuzin for valuable discussions. We gratefully acknowledge financial support by the Russian Science Foundation, project RSF-24-22-00060, <https://rscf.ru/project/24-22-00060/>

¹ Libor Šmejkal, Jairo Sinova, and Tomas Jungwirth, Phys. Rev. X 12, 031042 (2022)

² Igor Mazin, Phys. Rev. X 12, 040002 (2022); 10.1103/PhysRevX.12.040002

³ B.A. Volkov and O.A. Pankratov, JETP Lett., Vol. 42, No. 4, 178–181 (1985)

⁴ M. Z. Hasan and C. L. Kane: Colloquium: Topological insulators, Reviews of Modern Physics, Vol. 82, pp. 3045–3067 (2010)

⁵ N. P. Armitage, E. J. Mele, and Ashvin Vishwanath, Rev. Mod. Phys. 90, 15001 (2018)

⁶ Hai-Yang Ma, Mengli Hu, Nana Li, Jianpeng Liu, Wang Yao, Jin-Feng Jia and Junwei Liu, Nature Communications

- 12, 2846 (2021)
- ⁷ Noam Morali, Rajib Batabyal, Pranab Kumar Nag, Enke Liu, Qiunan Xu, Yan Sun, Binghai Yan, Claudia Felser, Nurit Avraham, Haim Beidenkopf, *Science*, Vol. 365, 6459, 1286 (2019)
- ⁸ Sultan Albarakat1, Cheng Tan1, Zhong-Jia Chen, James G. Partridge, Guolin Zheng, Lawrence Farrar, Edwin L.H. Mayes, Matthew R. Field, Changgu Lee, Yihao Wang, Yiming Xiong, Mingliang Tian, Feixiang Xiang, Alex R. Hamilton, Oleg A. Tretiakov, Dimitrie Culcer, Yu-Jun Zhao, Lan Wang, *Sci. Adv.* 5, eaaw0409 (2019).
- ⁹ Jabir Ali Ouassou, Arne Brataas, Jacob Linder, *Physical Review Letters* 131, 076003 (2023); <https://doi.org/10.1103/PhysRevLett.131.076003>
- ¹⁰ Z. Feng, X. Zhou, L. Šmejkal, L. Wu, Z. Zhu, H. Guo, R. González-Hernández, X. Wang, H. Yan, P. Qin, X. Zhang, H. Wu, H. Chen, Z. Xia, C. Jiang, M. Coey, J. Sinova, T. Jungwirth, and Z. Liu, *Nat. Electron.* 5, 735 (2022).
- ¹¹ Igor I. Mazin arXiv:2203.05000
- ¹² Sachchidanand Das, Dhavala Suri, Abhiram Soori, *J. Phys. : Condens. Matter* 35, 435302 (2023), <https://doi.org/10.1088/1361-648X/acea12>
- ¹³ Rui Chen, Zi-Ming Wang, Hai-Peng Sun, Bin Zhou, Dong-Hui Xu, arXiv:2501.14217
- ¹⁴ L. Šmejkal, R. González-Hernández, T. Jungwirth, and J. Sinova., *Science Advances* 6, eaaz8809 (2020).
- ¹⁵ R.D. Gonzalez Betancourt, J. Zubac, R. Gonzalez-Hernandez, K. Geishendorf, Z. Soban, G. Springholz, K. Olejnik, L. Smejkal, J. Sinova, T. Jungwirth, S.T.B. Goennenwein, A. Thomas, H. Reichlova, J. Zelezny, and D. Kriegner, *Phys. Rev. Lett.* 130, 036702 (2023).
- ¹⁶ K. P. Kluczyk, K. Gas, M. J. Grzybowski, P. Skupiński, M. A. Borysiewicz, T. Fas, J. Suffczyński, J. Z. Domagala, K. Graszka, A. Mycielski, M. Baj, K. H. Ahn, K. Výborný, M. Sawicki, M. Gryglas-Borysiewicz, *Physical Review B* 110, 155201 (2024)
- ¹⁷ Miina Leiviskä, Javier Rial, Antonín Badura, Rafael Lopes Seeger, Ismaila Kounta, Sebastian Beckert, Dominik Kriegner, Isabelle Joumard, Eva Schmoranzzerová, Jairo Sinova, Olena Gomonay, Andy Thomas, Sebastian T.B. Goennenwein, Helena Reichlová, Libor Šmejkal, Lisa Michez, Tomáš Jungwirth, Vincent Baltz *Phys. Rev. B* 109, 224430 (2024)
- ¹⁸ Satoru Hayami and Hiroaki Kusunose, *Phys. Rev. B* 103, L180407 (2021).
- ¹⁹ Merce Roig, Yue Yu, Rune C. Ekman, Andreas Kreisel, Brian M. Andersen, Daniel F. Agterberg, arXiv:2412.09338
- ²⁰ Lulu Li, Junwen Sun, Lei Wang, X. R. Wang, Ke Xia, arXiv:2412.06630
- ²¹ I. I. Mazin *Phys. Rev. B* 107, L100418 (2023)
- ²² K. D. Belashchenko, arXiv:2407.20440
- ²³ Vladimir A. Zyuzin, arXiv:2412.13009
- ²⁴ D. Kriegner, K. Výborný, K. Olejnik, H. Reichlová, V. Novák, X. Marti, J. Gazquez, V. Saidl, P. Němec, V. V. Volobuev, G. Springholz, V. Holý, and T. Jungwirth, *Nat. Commun.* 7, 11623 (2016).
- ²⁵ S. Greenwald, *Acta Crystallogr.* 6, 396 (1953).
- ²⁶ T. Komatsubara, M. Murakami, and E. Hirahara, *J. Phys. Soc. Jpn.* 18, 356 (1963).
- ²⁷ N. Kunitomi, Y. Hamaguchi, and S. Anzai, *J. Phys. (Les Ulis, Fr.)* 25, 568 (1964).
- ²⁸ M. Podgorny and J. Oleszkiewicz, *J. Phys. C* 16, 2547 (1983).
- ²⁹ E. Przedzińska, E. Kaminska, E. Dynowska, R. Butkute, W. Dobrowolski, H. Kepa, R. Jakiela, M. Aleszkiewicz, E. Lusakowska, E. Janik, and J. Kossut, *Phys. Status Solidi C* 2, 1218 (2005).
- ³⁰ Komatsubara Takemi, Murakami Miyuki, Hirahara Eiji, *Journal of the Physical Society of Japan*, Volume 18, Issue 3, pp. 356-364 (1963). DOI:10.1143/JPSJ.18.356
- ³¹ D. Kriegner, H. Reichlova, J. Grenzer, W. Schmidt, E. Ressouche, J. Godinho, T. Wagner, S. Y. Martin, A. B. Shick, V. V. Volobuev, G. Springholz, V. Holy, J. Wunderlich, T. Jungwirth, and K. Vyborny, *Phys. Rev. B* 96, 214418 (2017) DOI: 10.1103/PhysRevB.96.214418
- ³² N.N. Orlova, A.A. Avakyants, A.V. Timonina, N.N. Kolesnikov, and E.V. Deviatov, *JETP Letters*, 120, 360 (2024). <https://doi.org/10.1134/S0021364024602926>
- ³³ A. A. Avakyants, N. N. Orlova, A. V. Timonina, N. N. Kolesnikov and E. V. Deviatov, *JETP Lett.* 119, 625 (2024). <https://doi.org/10.1134/S0021364024600605>
- ³⁴ Hooqboom, G. (2021). Spin transport and spin dynamics in antiferromagnets. [Thesis fully internal (DIV), University of Groningen]. University of Groningen. <https://doi.org/10.33612/diss.157444391>
- ³⁵ X. Sun, E. Feng, Y. Su, K. Nemkovski, O. Petravic, T. Brückel, *J. Phys.: Conf. Ser.* 862 012027 (2017)
- ³⁶ Y.P. Zhu, X. Chen, X.R. Liu, Y. Liu, P. Liu, H. Zha, G. Qu, C. Hong, J. Li, Z. Jiang, X.M. Ma, Y.J. Hao, M.Y. Zhu et al., *Nature* 626, 523 (2024). <https://doi.org/10.1038/s41586-024-07023-w>
- ³⁷ Sang-Wook Cheong, Fei-Ting Huang, *npj Quantum Mater.* 9, 13 (2024) <https://doi.org/10.1038/s41535-024-00626-6>
- ³⁸ A. Hariki, A. Dal Din, O. J. Amin, T. Yamaguchi, A. Badura, D. Kriegner, K. W. Edmonds, R. P. Champion, P. Wadley, D. Backes, L. S. I. Veiga, S. S. Dhési, G. Springholz, L. Smejkal, K. Vyborny, T. Jungwirth, J. Kunes, *Phys. Rev. Lett.* 132, 176701 (2024)
- ³⁹ M. Hajlaoui, S.W. D'Souza, L. Smejkal, D. Kriegner, G. Krizman, T. Zakusylo, N. Olszowska, O. Caha, J. Michalička, A. Marmodoro, K. Výborný, A. Ernst, M. Cinchetti, J. Minar, T. Jungwirth, G. Springholz, *Adv. Mater.* 36, 2314076 (2024)
- ⁴⁰ T. Osumi, S. Souma, T. Aoyama, K. Yamauchi, A. Honma, K. Nakayama, T. Takahashi, K. Ohgushi, and T. Sato, *Phys. Rev. B* 109, 115102 (2024)
- ⁴¹ A. S. Borovik-Romanov *JETP*, 9, 539 (1959)
- ⁴² I. Dzyaloshinsky, *J. Phys. Chem. Solids*, 4(4), 241-255 (1958)
- ⁴³ Libor Smejkal, Jairo Sinova, and Tomas Jungwirth, *Phys. Rev. X* 12, 040501 (2022). DOI: <https://doi.org/10.1103/PhysRevX.12.040501>